Reprint 561

Applications of Radar-based Nowcasting Techniques for Mesoscale Weather Forecasting in Hong Kong

P.W. Li & E.S.T. Lai

Meteorological Applications Vol. 11, pp 253-264, 2004

Meteorol. Appl. 11, 253–264 (2004) DOI:10.1017/S1350482704001331

Applications of radar-based nowcasting techniques for mesoscale weather forecasting in Hong Kong

P. W. Li & Edwin S. T. Lai
Hong Kong Observatory, 134A Nathan Road, Kowloon, Hong Kong
Email: pwli@hko.gov.hk

Operational forecasting of mesoscale weather systems in Hong Kong is supported by an automated nowcasting system called SWIRLS (Short-range Warning of Intense Rainstorms in Localised Systems). SWIRLS is based on the extrapolation of radar echoes using the TREC (Tracking Radar Echoes by Correlation) technique. With a suitable choice of pixel array size on the radar reflectivity maps, the TREC vectors derived can be used to monitor and extrapolate echo motion right across the mesoscale spectrum, from individual convective cells, to supercells and clusters, and to groups of rainbands or squall lines.

On the basis of TREC, quantitative precipitation forecast (QPF) algorithms have been developed to produce high resolution forecast rainfall distribution maps over the local area. These maps provide useful objective guidance for forecasters to assess the likely rain scenario in the next few hours and to facilitate decision-making in operating the Rainstorm Warning System. This review, however, will focus on other aspects of TREC applications and some side benefits for operational mesoscale forecasting in Hong Kong. First, extension of the TREC technique to group tracking of echoes (GTrack) have enabled forecasters to make qualitative educated guesses of the likelihood of prolonged heavy rain or the potential of enhanced storm development. Secondly, extension of the QPF algorithms to a forecast range of 3 hours, supplemented by real-time accumulated rainfall data from a high density raingauge network, has enabled forecasters to provide reliable advice and guidance to geotechnical engineers for landslip risk assessment. Thirdly, rain-related applications aside, TREC vectors are also ingested into a data analysis system LAPS (Local Analysis and Prediction System) adapted from Forecast Systems Laboratory (FSL) of NOAA. Through the assimilation of TREC vectors and other wind observations, a three-dimensional wind structure of tropical cyclones can be generated in near real-time for forecasters' reference in assessing landfall impact.

1. Introduction

Although NWP models are becoming more sophisticated and new computers are getting more powerful, many modellers would readily acknowledge that mesoscale weather systems are yet to be simulated with satisfactory results (e.g. Crook 1996). One of the reasons is the complex physical processes involved. The sensitivity of the non-linear physical equations to the initial conditions complicates matters as well. Another obstacle is the lack of a suitable data assimilation scheme that can fully utilise remote sensing observations of ultra-fine resolution, on spatial and temporal scales.

Nowcasting, in contrast, is by definition a collection of very short-range forecasting techniques that starts from a 'detailed description of the current weather', made possible by fully utilising all observations available, in particular remote sensing data from radar, satellite, wind profiler, GPS, etc. (e.g. Browning 1982, Conway 1998). Nowcasting thus plugs the gap in NWP where it has lower skill, i.e. in the first few hours of the model run when model performance has not yet stabilised. This is also the forecast range when forecasters often have to make critical operational decisions in the face of rapidly developing weather situations. Nowcasting capability has therefore become an increasingly important and specialised subject that affects daily forecasting operations as well as decision-making processes in weather services (Liljas, 1998).

Among all the mesoscale weather systems that affect sub-tropical regions such as Hong Kong, rainstorms and tropical cyclones have the greatest impact. Rainstorms in Hong Kong, modulated by hilly terrain and tortuous coastlines, can occur in association with local convergence effects, active monsoon, troughs of low pressure, frontal systems, as well as the spiral rainbands of tropical cyclones. They bring flash floods to the territory, endangering lives and properties and creating general chaos. The Hong Kong Observatory (HKO) has been operating a Rainstorm Warning System (RWS) since the early 1980s in a bid to give the local community early warning of such rain events. After several adjustments along the way, the current RWS is based on a three-tiered colour scheme of amber, red and black, corresponding to hourly rainfall amounts of 30 mm, 50 mm and 70 mm respectively over a wide area. Over a 20-year period from 1983 to 2002, the annual average occurrences of amber, red and black rainstorms are respectively 30, 5 and 1.

In support of the RWS operation, HKO has developed a nowcasting system called SWIRLS (Short-range Warning of Intense Rainstorm in Localised Systems). Phase I of the system, mainly QPF (quantitative precipitation forecasts) based on the processing of TREC (Tracking Radar Echoes by Correlation) vectors and reanalysed radar-raingauge rainfall data, was completed and put into operation in 1998. The TREC module traces the movement of an array of reflectivity pixels between two successive radar images (Tuttle & Foote 1990), a time interval of 6 minutes in the case of the HKO radar. The original design is to provide real-time QPF estimation for the following two hours, updated every 6 minutes, through the extrapolation of echo movement using the derived TREC vectors. Detailed description of SWIRLS and the QPF aspects are reported in Li & Lai (2004).

After several years of operation, local forecasters have gained some experience in the use of SWIRLS and new ideas have evolved on the practical application of the system in an operational environment. This paper focuses on some extended applications of SWIRLS in association with the forecasting of mesoscale weather. Section 2 reports on the use of TREC and GTrack (Group Tracking), a supplementary module for tracking radar echo groups, for qualitative assessment of rainstorm development. Section 3 sees the QPF algorithms extended to produce 3-hour forecasts in support of landslip risk assessment with good effect. Section 4 describes the use of TREC vectors in near real-time tropical cyclone wind analyses. Concluding remarks and discussions are presented in Section 5.

2. Qualitative rainstorm risk assessment

SWIRLS has two echo movement modules, namely TREC and GTrack. The two components are meant to complement each other for a more complete description of echo motion. As explained in Li & Lai (2004), the TREC vectors are derived from the matching of pixel arrays (boxes) between two successive radar images through maximum cross-correlation. With a suitably chosen box size, the TREC module can reveal the motion of echoes on different spatial scales, including the inner structure of the target rainstorm. GTrack, on the other hand, groups the pixels over some predefined intensity threshold in the form of an ellipse and tracks the movement of ellipse centroids between successive radar images. In other words, GTrack is an 'object-oriented' technique for tracking the movement of a storm as a whole entity.

2.1. A red rainstorm case

Figure 1 shows the 128-km range, 3-km height TREC wind analyses of a rainstorm event in Hong Kong on 12 June 2001. The gridded TREC wind vectors in this example have a horizontal separation of about 2.5 km. While most of the TREC vectors are pointing to the northeast, two distinct rain systems, labelled 'A' and 'B', can be readily identified (subjectively) by grouping the neighbouring but similar TREC vectors. System 'A' aligned in a zonal direction moved northeastwards at about 20 km/hr. The relatively slow movement of this system was a manifestation of the convergence of the continental air mass over the mainland to the north and a maritime airstream from the south. On the other hand, system 'B', aligned along a meridional direction in association with a propagating perturbation in the upper westerlies, was sweeping northeastwards at a much faster speed of about 40 km/hr.

The common notion that rain intensity would be enhanced when storms merge or when rainbands intersect one another (e.g. Wilson & Mueller 1993) was also observed in this case. Figure 2a shows the rainfall distribution registered by the network of raingauges within the Hong Kong territory between 3 a.m. and 4 a.m. that morning. Figure 2b shows the SWIRLS 1-hour QPF for the same period. Numbers plotted on the map are forecast rainfall values interpolated to the actual raingauge locations; and for illustration purposes, 'bogus' gauges over the sea areas used for the analysis and plotting routines are also shown. Areas of heavier rain are shaded, revealing a good resemblance to the actual situation in Figure 2a.

While TREC-based QPF in general offers reliable nowcasting guidance in the course of this particular event, the GTrack module, to a certain extent, was also able to depict the interaction between systems 'A' and 'B'. By using a reflectivity threshold of 34 dBZ, a number of ellipses can be identified in the GTrack module (Figure 3). Ellipses A1 to A5 in Figure 3 are obviously associated with their counterpart system 'A' in Figure 1; while B1 and B2 are associated with their counterpart system 'B'. Based on their respective movements in the previous 12 minutes, a motion vector (called GTrack vector) could be calculated for each of the ellipses. Linear extrapolation of the ellipse centroids associated

(a)

(b)

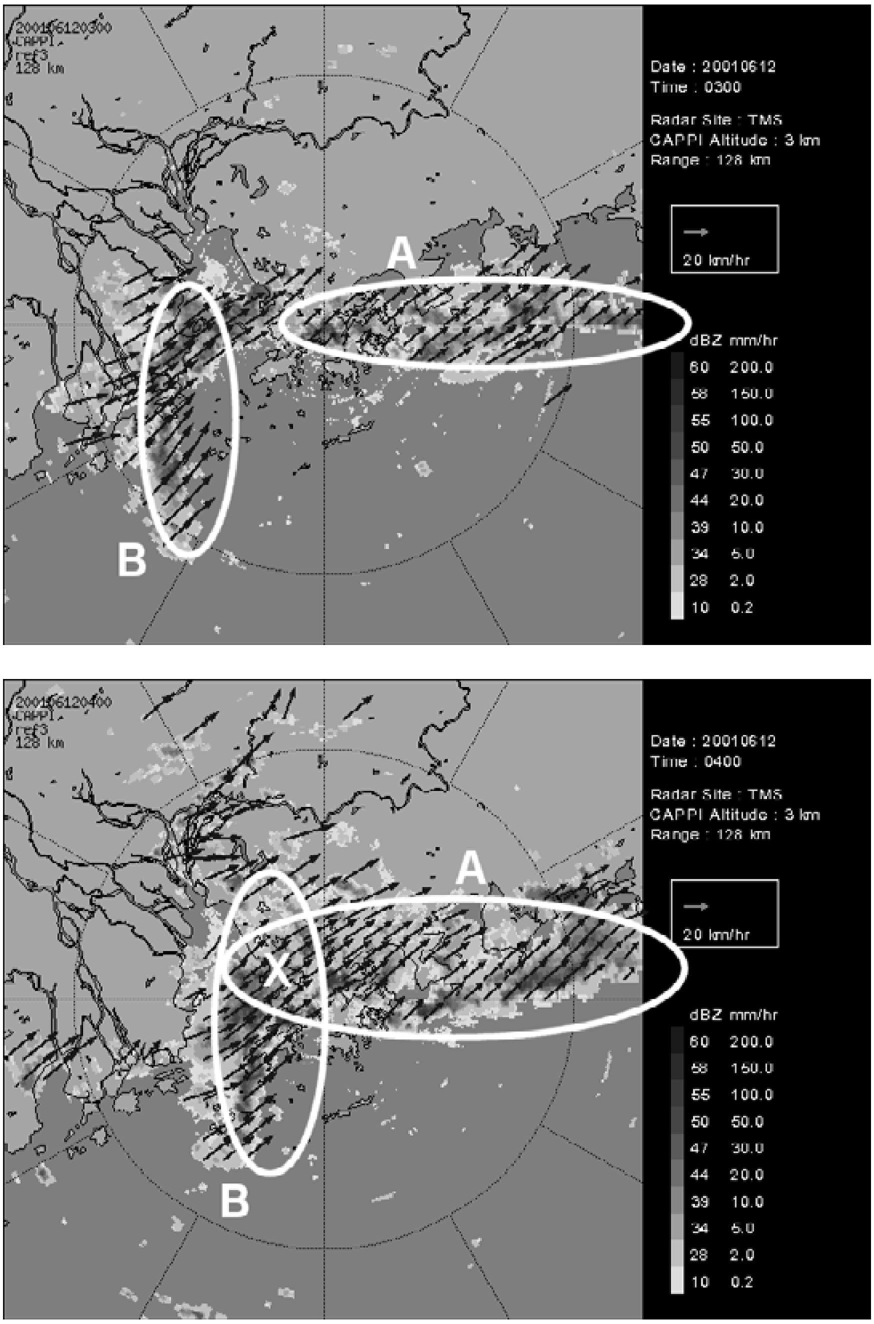

Figure 1. *TREC wind analyses (at 3-km level) of a rainstorm event on 12 June 2001: (a) at 3:00 HKT; (b) at 4:00 HKT. (Note: HKT = UTC + 8 hours.)*

with B1 and B2 along their respective GTrack vectors clearly suggested possible collision and merging with the slow-moving storm systems such as A1 and A2 lingering along the coastline.

2.2. A hailstorm case

By increasing the spatial resolution in the correlation algorithm, TREC can also reveal the finer structure of a severe storm such as a supercell. Figure 4 shows the 64-km range, 3-km height TREC analyses of a hailstorm event on 9 April 2001. The horizontal resolution of the gridded TREC vectors in this case is 1.2 km. In Figure 4a, system 'A' was generally moving southeastwards and system 'B' had a mean flow pointing to the east-northeast. Just as in Section 2.1, the collision of the two systems resulted in further storm enhancement at a later time. But some tell-tale features in the TREC fields could be found in connection with system 'A'. Originating from a core of maximum reflectivity of about 60 dBZ over the northwestern corner of the map, the TREC vectors appeared to converge towards a focus labelled X (Figure 4a). This converging feature remained evident in successive images, lasting for nearly half an hour when the storm was at its most intense.

A couple of hours later, similar features were again found as the storm complex swept across Hong Kong.

(a)

(b)

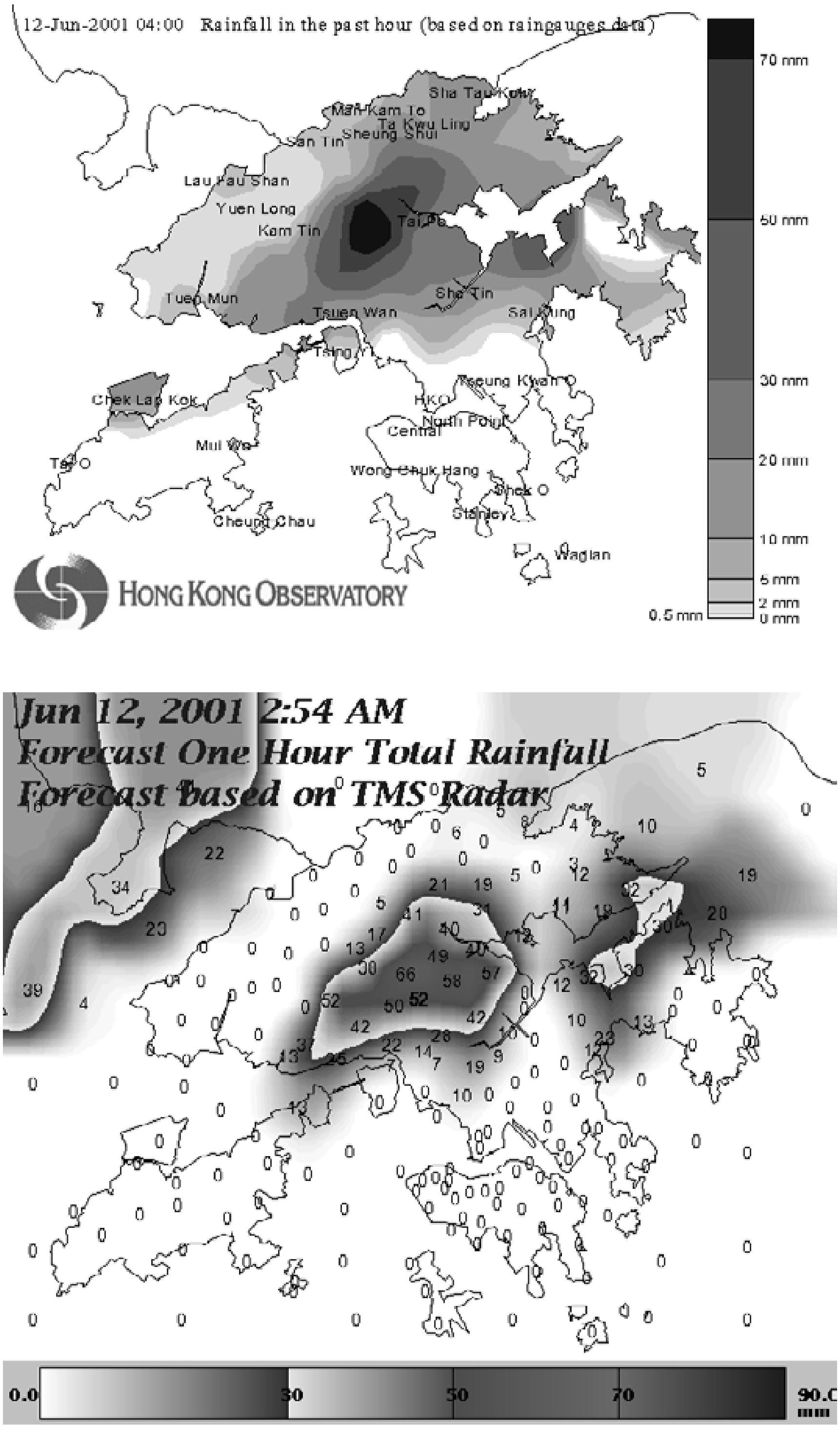

Figure 2. *Verification of SWIRLS QPF for the rainstorm shown in Figure 1: (a) hourly accumulated rainfall recorded by raingauges between 3:00 and 4:00 HKT; (b) SWIRLS QPF at 2:54 HKT for the following hour.*

TREC vectors south of the line C–C' converged towards an area marked X' in Figure 4b. Vertical cross-section of the supercell along line C–C' (Figure 5) reveals a typical overhang feature normally associated with hailstorms and a bounded weak echo region (BWER) below the maximum core. As hypothesised in many classical conceptual models (see, for example, Browning & Foote 1976), a trail of hailstones was found to the left of the BWER at the surface.

One possible explanation for the TREC vector convergence is the tendency of the northwesterlies to go around the mesocyclone at the core of the supercell, converging towards the front flank downdraft, sinking below and undercutting the on-rushing southwesterlies. Geometrically speaking, this corresponds to the bending of a multicell squall line into a curvilinear comma shape ('hook echoes' or 'bow echoes'). This is particularly noticeable for system 'A' in Figure 4a. If such a

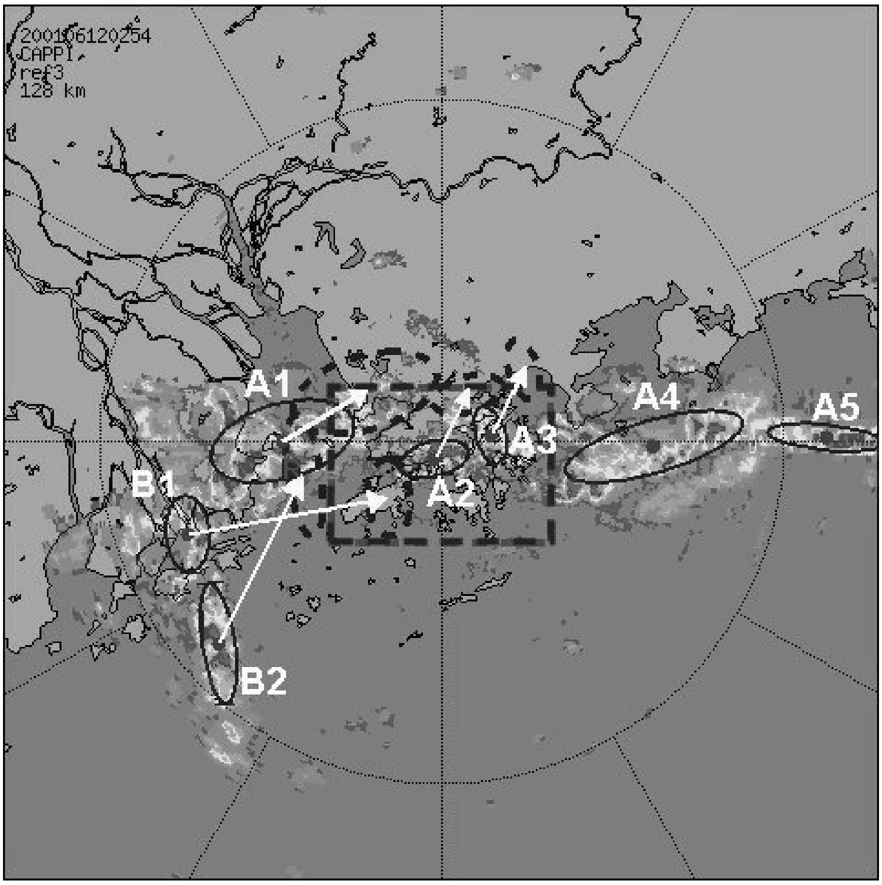

Figure 3. *GTrack analysis at 2:54 HKT on 12 June 2001 for the same rainstorm event shown in Figure 1. Ellipses with solid line are the present positions and those with dashed line the respective forecast positions one hour later. Arrows are the predicted movements of the respective ellipses. Apart from those two ellipses on the right hand side with insufficient information to do an extrapolation, all other forecast ellipses' positions congregate around the Hong Kong region (the dashed rectangular box).*

hypothesis is valid, then the TREC vector convergence feature is potentially a useful signature for hailstorm identification.

3. Objective landslip risk assessment

Apart from RWS that focuses on intense rain of short duration, HKO is also operating a Landslip Warning System (LWS) in collaboration with the Geotechnical Engineering Office (GEO). The LWS was developed in the early 1970s after some major landslide disasters in Hong Kong as a result of prolonged and extensive heavy rain. The original design was based solely on actual observations, by statistically relating the number of landslips with the 24-hr cumulative rainfall. Since 2000, a forecast component has been introduced, whereby the 24-hr accumulated rainfall used for assessing the risk of landslips is constructed from (a) 21-hr 'observed' rainfall from the raingauges, and (b) 3-hr QPF from SWIRLS. As explained in Li & Lai (2004), estimation of rainfall distribution in the next 3 hours is simply an extended extrapolation of echo movement along the TREC vectors.

Apart from the introduction of a forecasting element, the new LWS also incorporates a concept called 'Vulnerable Area' (VA) for assigning different weightings to different raingauges. To put it simply, raingauges at locations that have a long history of landslip occurrences are assigned larger weightings than those with fewer historical occurrences. The number of likely landslip occurrences for each raingauge under a rain event is then derived through statistical correlation. By including the VA weighting factor for each raingauge, SWIRLS will automatically trigger a LWS alarm if the sum of likely landslips from all the contributing raingauges exceeds a predetermined threshold criterion, currently set at 15. As the QPF guidance is updated every 6 minutes, forecasters are immediately alerted to possible LWS risks as the rain event unfolds and GEO staff promptly informed accordingly. To illustrate how SWIRLS works in the context of LWS, the two rainfall distribution maps in Figure 6 for a rain event in the evening of 1 September 2001 are merged to produce a forecast 24-hr accumulated rainfall map valid at T + 3 hour (i.e. at 1 a.m. on 2 September 2001). The total number of landslips predicted was over 15 and a LWS alarm was triggered at that particular time.

The histogram in Figure 7 plots the number of SWIRLS LWS alarm occurrences as a function of lead time before the warning criterion is actually reached. In 2001 and

(a)

(b)

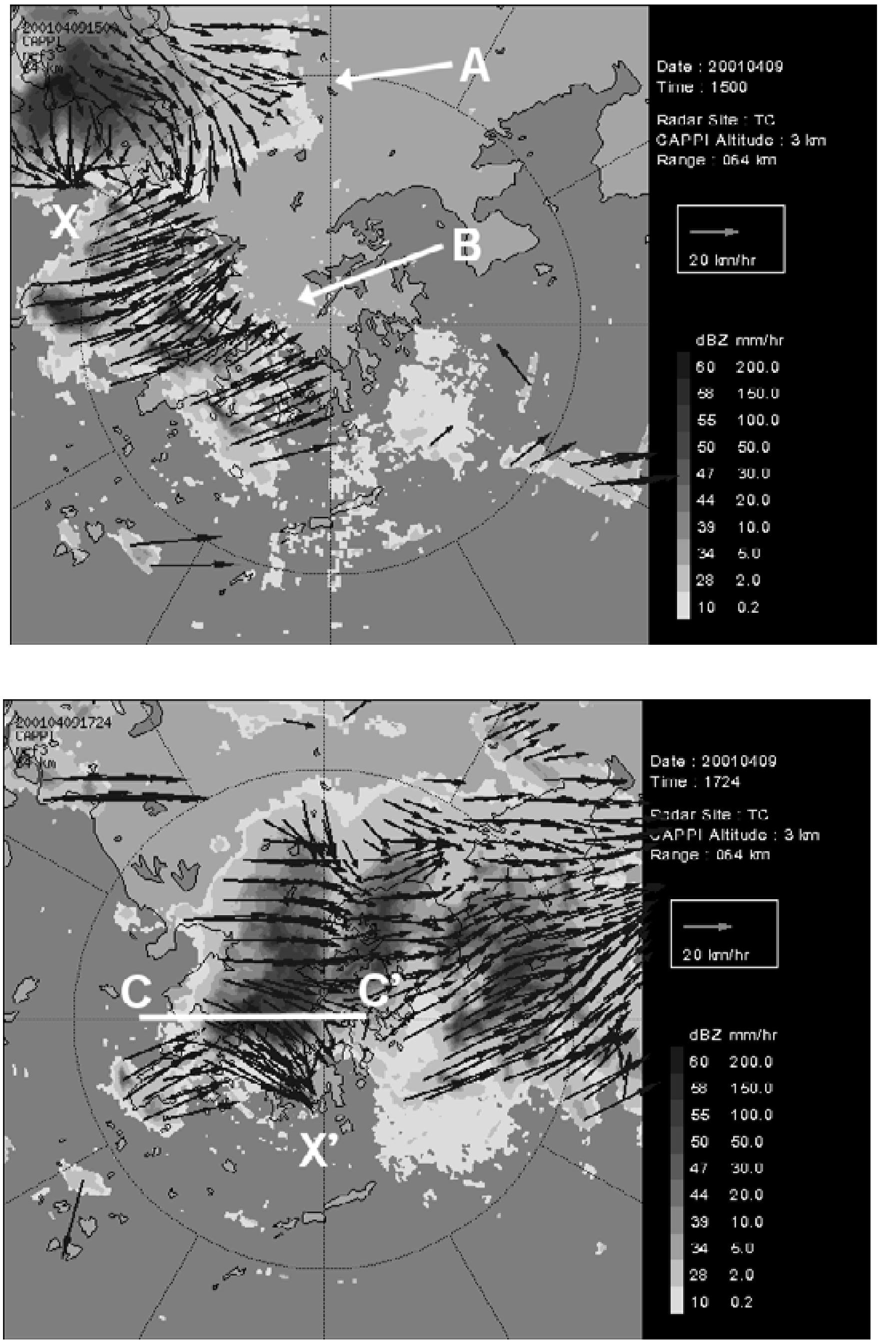

Figure 4. *64-km range, 3-km height TREC vector analysis of a hailstorm on 9 April 2001: (a) at 15:00 HKT; and (b) at 17:24 HKT.*

2002, SWIRLS issued 13 LWS alarms, of which 12 were verified to be correct and 1 was a false alarm. In the same period, there were actually 14 cases of rainfall reaching landslip warning criteria. Among them, 12 were forecast by SWIRLS with lead times of 4 hours or less while two cases were missed (taken to be negative lead time in the histogram). Typically, the SWIRLS LWS lead time is between 1 and 2 hours, with an average value of 1.2 hours. Figure 8 is the contingency table for the same set of verification data. The POD (probability of detection) and the FAR (false alarm rate) are respectively 0.86 and 0.08. As such, the CSI (Critical Success Index; Wilks 1995) is as high as 0.80. All the indices suggest that the SWIRLS LWS application is sufficiently robust in providing reliable guidance for objective landslip risk assessment.

4. Tropical cyclone wind field analyses

Conventional methods for analysing the intensity of a tropical cyclone is mostly based on the Dvorak method (Dvorak 1975) in conjunction with available surface observations. For a more complete description of the cyclone structure, in particular the wind fields associated with the cyclone circulation, remote sensing techniques offer the most promising prospect. In recent years, new observation platforms such as the

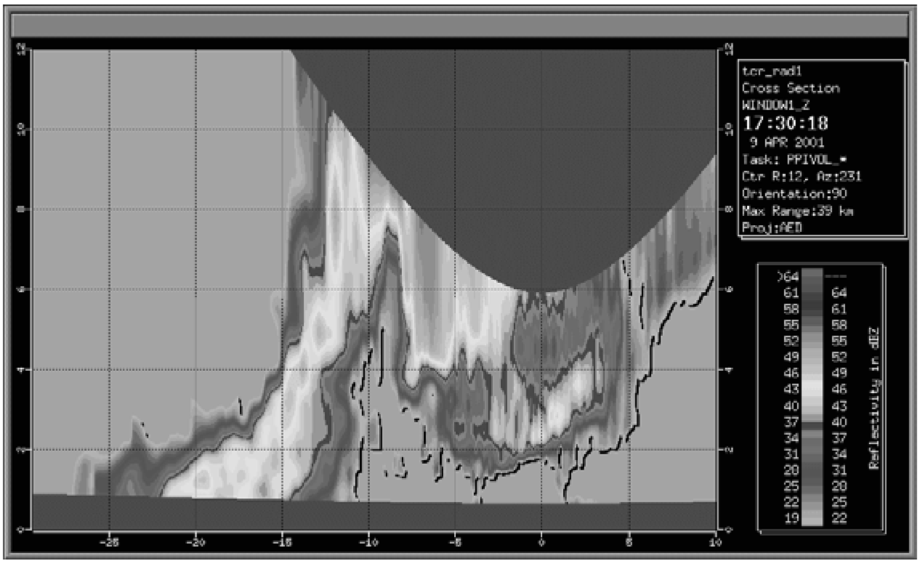

Figure 5. *Vertical cross-section along the line C–C' in Figure 4b at 17:30 HKT.*

QuikSCAT satellite have provided near-surface wind information when a tropical cyclone is over the open seas. For tropical cyclones approaching land, Doppler radar offers more continuous monitoring. It also has the advantage of providing data coverage at very high spatial and temporal resolution. While single or dual Doppler wind retrievals are the obvious options, Lai (1998) and Tuttle & Gall (1999) have also demonstrated the use of the TREC technique in analysing the wind structure of tropical cyclones over the South China Sea and North Atlantic basins respectively.

Encouraged by such results, it is hoped that the evolution of the three-dimensional wind structure of tropical cyclones can be studied in near real-time through a rapidly updated data analysis system that can ingest TREC vectors as well as wind observations from a variety of alternative data sources such as QuikSCAT, wind profiler, Doppler winds, SATOBS, etc.

The data analysis system used for this investigation is the Local Analysis and Prediction System (LAPS) of the Forecast Systems Laboratory of NOAA. LAPS is flexibly designed for ingestion of virtually all kinds of conventional as well as remote-sensing data (Albers 1995; Albers et al. 1996). In HKO's implementation, the first-guess wind field is obtained from HKO's 20-km resolution ORSM (Operational Regional Spectral Model) (NPD/JMA 1997). TREC vectors for tropical cyclones within the radar range are computed and assimilated into LAPS along with other available wind observations. Table 1 is a summary of the observational data currently ingested into LAPS, along with some background information on ORSM for reference.

Figure 9 is an example of the 1-km height 256-km range TREC analysis of Typhoon Utor, which moved north-northwestwards across the coast of southern China on 6 July 2001. The vortex circulation and the echo movement along its outer rainband are in general well depicted by TREC. It can be seen that the TREC vectors on the eastern sector of the cyclone circulation have higher wind speeds, consistent with the commonly observed tendency that winds to the right of the storm track are generally stronger.

Table 1. *Characteristics of LAPS and ORSM implemented by HKO.*

	LAPS	
3-hourly wind observations	SYNOPS, SHIP, BUOY, Wind Profiler, AMDAR, radiosonde, SATOBS	
Additional hourly wind observations	AWS, METAR, AMDAR, Profiler winds, Doppler radar winds, TREC winds	
Non-regular hours wind observations	QuikSCAT	
Horizontal resolution	5 km	
Vertical resolution	50 hPa	
Analysis scheme	Successive correction	
First Guess	20-km ORSM wind field	
	ORSM	
Horizontal resolution	20 km	60 km
No. of vertical levels	36	36
No. of grid points	151×145	151×145
Domain coverage	10–35°N 100–128°E	9°S–59°N 65–152°E
Initial condition	20-km ORSM analysis	60-km ORSM analysis
Boundary condition	60-km ORSM forecasts	JMA's GSM forecasts

Figure 10 shows the 900-hPa LAPS analysis of Utor before and after landfall. The horizontal resolution is 5 km and the vertical resolution 50 hPa. Just before landfall (Figure 10a), the analysis indicates that the wind structure of Utor is rather asymmetric. Winds to the

(a)

(b)

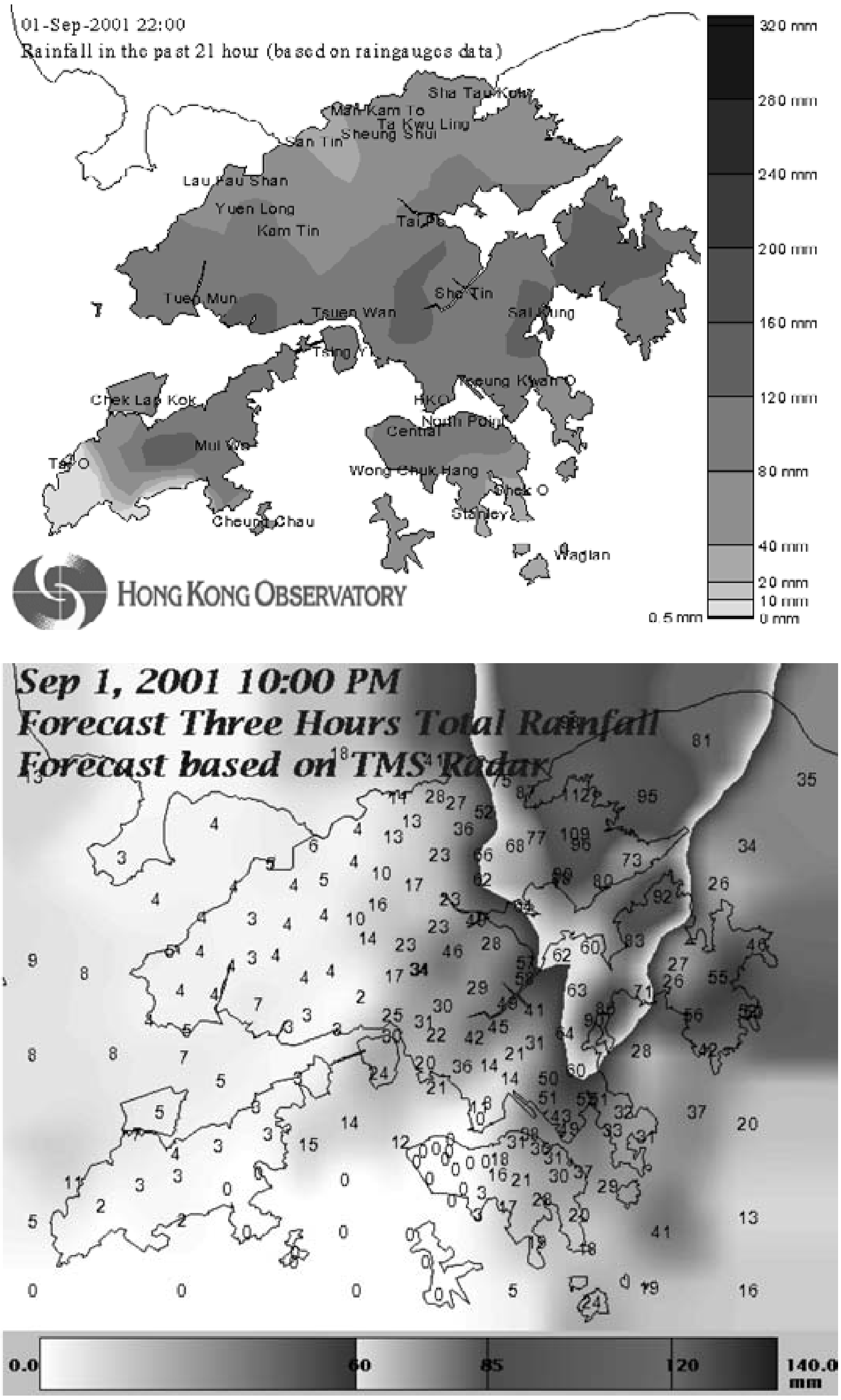

Figure 6. *(a) Previous 21-hr accumulated rainfall recorded at the raingauges at 22:00 HKT on 1 Sep 2001; (b) SWIRLS 3-hr QPF effective from 22:00 HKT on the same day.*

south over the sea areas have a maximum speed of 80 knots (i.e. about 150 km/hr) while the winds to the north over land are much weaker with a maximum speed of 30 knots (i.e. about 55 km/hr) only. After landfall (Figure 10b), the circulation becomes more symmetric, with winds to the south dropping to about 50 knots (i.e. about 90 km/hr) while winds over the northwestern quadrant have increased to roughly the same magnitude. Another interesting observation after landfall is the apparent outward expansion of the radius of maximum winds away from the eye region, a sign of general weakening. This is corroborated by local wind trends in Hong Kong, with winds actually becoming much stronger well after the passage of the eye. The importance of radar data, including the radar Doppler wind and TREC wind, can be revealed by comparing the LAPS analysis with radar data ingested to that without radar data ingested (not shown). It is found that without radar data incorporated the analysis results could only produce a tropical cyclone with the centre shifted and the wind field surrounding it weaker than that shown in Figure 10.

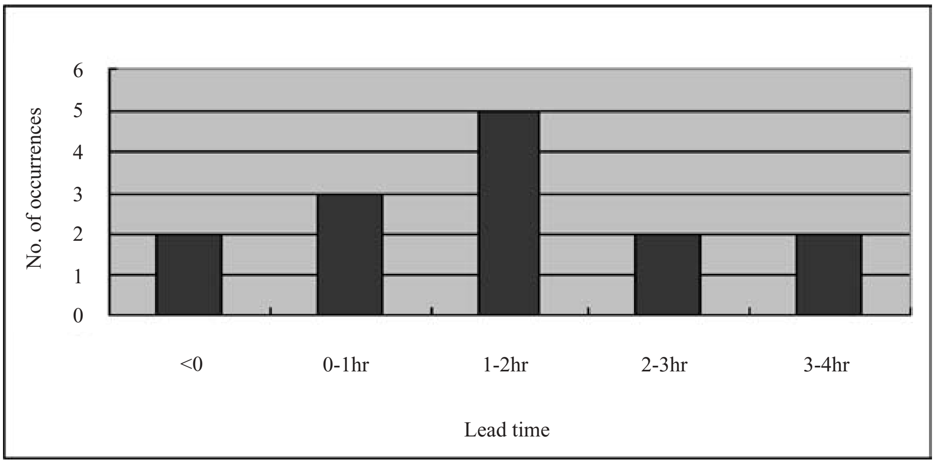

Figure 7. *Histogram showing number of SWIRLS LWS alarm occurrences in 2001 and 2002 as a function of lead time before warning criterion reached.*

Observed LW \ SWIRLS LW Forecast	Yes	No
Yes	12	2
No	1	–

Figure 8. *Contingency table of SWIRLS LWS verification for events in 2001 and 2002.*

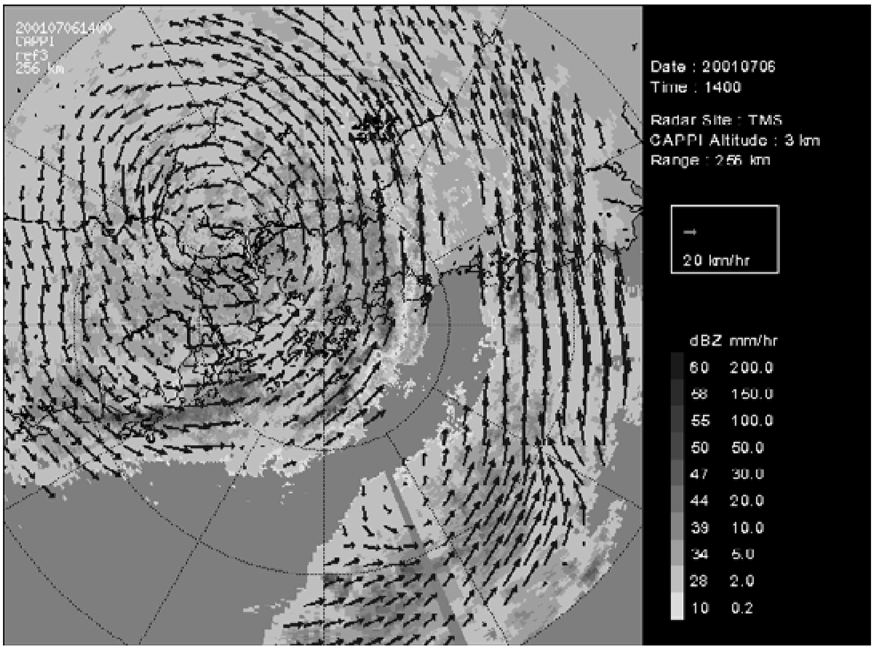

Figure 9. *1-km height 256-km range TREC analysis of Typhoon Utor affecting Hong Kong at 06 UTC on 6 July 2001.*

(a)
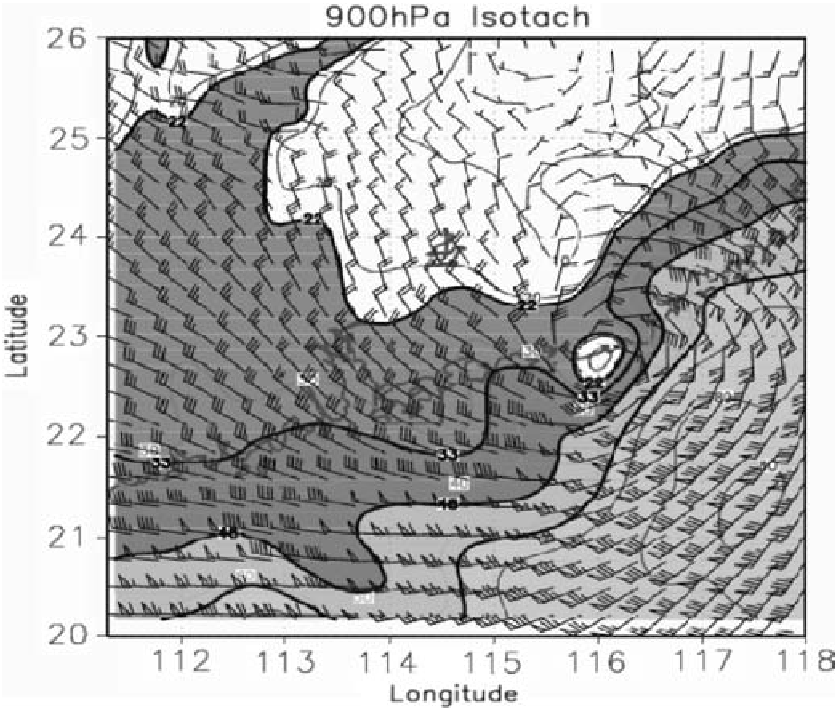

(b)
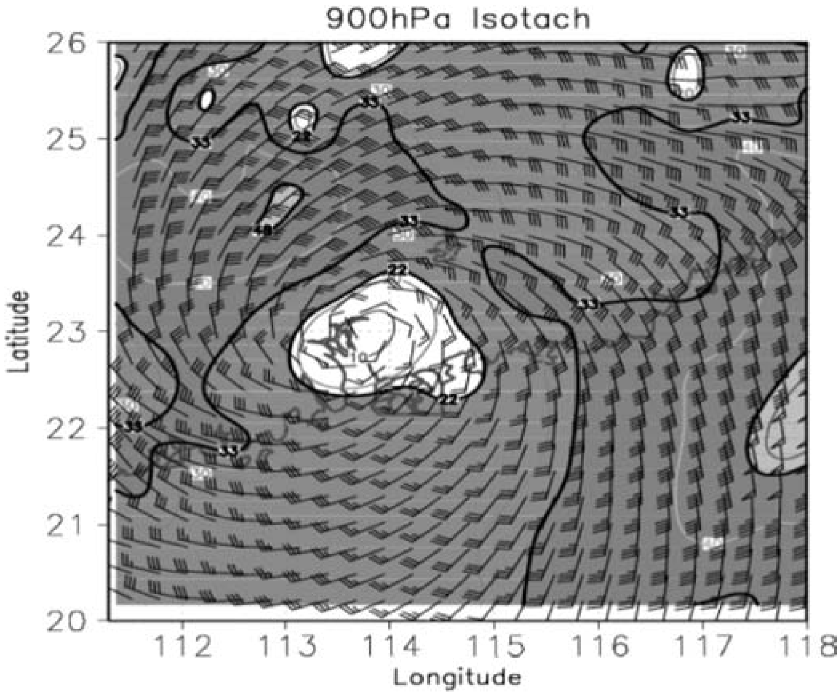

Figure 10. *900-hPa LAPS wind analysis of Typhoon Utor on 6 July 2001 at (a) 00 UTC and (b) 06 UTC. Shaded areas correspond to wind speeds of: 22–32 knots (medium gray), 33–47 knots (dark gray), 48–62 knots (light gray) and 63 knots or above (off white).*

In addition to the plan views of Utor in Figure 10, an in-depth look at Utor's vertical structure just before landfall as depicted by LAPS along a north–south plane through the eye is shown in Figure 11. While Figure 10a seemingly suggests relatively subdued winds at the 900-hPa level north of the eye, Figure 11 actually paints a rather different picture, showing an elevated core of isotach maximum near the 700-hPa level, accompanied by a secondary core much nearer the surface. While such detailed LAPS-analysed features have yet to be reliably verified, it does highlight the importance of looking at the complete 3-D structure and not the winds at any single level when estimating the intensity of the tropical cyclone. This is particularly relevant during cyclone landfall when vertical changes and transport of momentum through the lower troposphere and the boundary layer may play an important role in determining the gustiness, and hence wind damage, experienced at the surface.

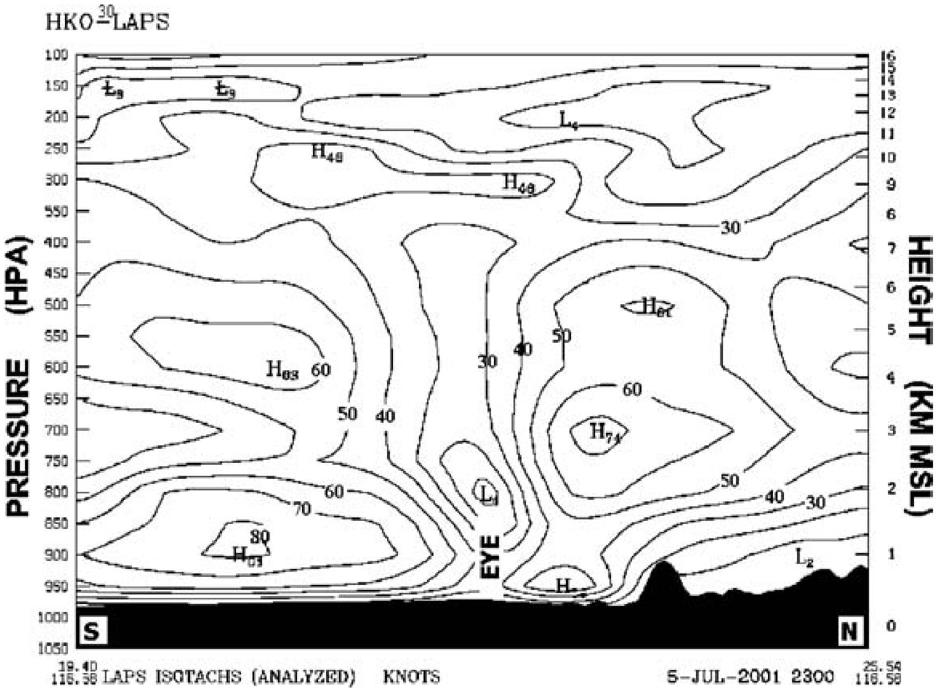

Figure 11. *North–south vertical cross-section of wind speed passing through the centre of Typhoon Utor at 00 UTC on 6 July 2001.*

5. Concluding remarks

In this paper, it has been demonstrated that various analysis and forecasting tools developed under the umbrella of SWIRLS can be applied with some success in operational monitoring and nowcasting of a whole spectrum of mesoscale weather systems, ranging from single-cell rainstorms, supercell thunderstorms, prolonged heavy rain episodes to tropical cyclones.

Extension of the TREC technique to group tracking of echoes (i.e. GTrack) have enabled forecasters to make qualitative educated guesses of the likelihood of prolonged heavy rain or the potential of enhanced storm development. Extension of the QPF algorithms to a forecast range of 3 hours, supplemented by real-time accumulated rainfall data from a high density raingauge network, has enabled forecasters to provide reliable advice and guidance to geotechnical engineers for landslip risk assessment. Through the assimilation of TREC vectors and other wind observations using a frequently updated data analysis system, a three-dimensional wind structure of tropical cyclones can be generated in near real-time for forecasters' reference in assessing landfall impact.

There are however some underlying limitations that restrict the applicability of a simple technique like TREC in different weather situations, even within the nowcasting range of just a few hours. The most obvious is the effect of combining TREC vectors across different spatial scales for echo movement extrapolation. The problem is non-trivial even for a single rain system, not to mention multiple systems interacting and merging. Similar considerations also apply in tropical cyclone cases. The TREC vectors derived are in fact a combination of the rotational movement of the spiral rainbands around the cyclone centre and the translational movement of the cyclone itself. It is difficult to separate the two components from a single set of TREC vectors. But until such time when a more sophisticated algorithm can be found and has proven its worth, the use of TREC in various SWIRLS applications provides simple yet useful guidance for operational forecasting decisions in the very short range.

Another limitation deserving attention relates to the interpretation of LAPS-analysed wind fields. Owing to the lack of reliable data near the surface, it will be difficult for LAPS to provide meaningful wind information below 1 km. Even if radar data below 1 km are available, the clutter problems associated with the hilly terrain of Hong Kong mean that the quality of TREC vectors so derived cannot be guaranteed. Until such time when more near-surface data are made available for ingestion, interpretation and use of LAPS-analyzed wind fields are best confined to levels above 1 km. For landfall impact at the surface, the recommended strategy is to make qualitative deductions based on implied intensity trends and changes through a sequence of consecutive LAPS analyses. Work is also underway to explore the possibility of using LAPS analysis as an alternative input to the initial conditions for non-hydrostatic models.

Acknowledgements

The authors would like to thank Mr C. Y. Lam for his stimulating ideas for the study and Messrs K. H.

Yeung and Y. K. Chan for reading the manuscript. The development work on the ingestion of TREC vectors into LAPS was completed with the assistance of Mr Philip K. Y. Chan and Dr Nathaniel T. Servando of the Philippine Atmospheric, Geophysical and Astronomical Services Administration (PAGASA). Dr Servando was attached to the Hong Kong Observatory under the support of the ESCAP/WMO Typhoon Committee Research Fellowship Scheme.

References

Albers, S., McGinley, J., Birkenheuer, D. & Smart, J. (1996) The Local Analysis and Prediction System (LAPS): analyses of clouds, precipitation, and temperature. *Wea. Forecasting* **11**: 273–287.

Albers, S. C. (1995) The LAPS wind analysis. *Wea. Forecasting* **10**: 342–352.

Browning, K. A. (1982) *Nowcasting.* London: Academic Press.

Browning, K. A. & Foote, G. B. (1976) Airfolow and hail growth in supercell storms and some implications for hail suppression, *Q. J. R. Meteorol. Soc.* **102**: 499–534.

Conway, B. J. (1998) An overview of nowcasting techniques. In *SAF Training Workshop – Nowcasting and Very Short Range Forecasting*, EUMETSAT.

Crook, N. A. (1996) Sensitivity of moist convection forced by boundary layer processes to low level thermodynamic fields. *Mon. Wea. Rev.* **124**: 1767–1785.

Dvorak, V. F. (1975) Tropical cyclone intensity analysis and forecasting from satellite imagery. *Mon. Wea. Rev.* **103**: 420–430.

Lai, E. S. T. (1998) TREC application in tropical cyclone observation. *ESCAP/WMO Typhoon Committee Annual Review 1998*, 135–139.

Li, P. W. & Lai, E. S. T. (2004) Short-range Quantitative Precipitation Forecasting in Hong Kong. *J. Hydrol.* **288**: 189–209.

Liljas, E. (1998) COST-78 co-operations on SAFs. In: *SAF Training Workshop – Nowcasting and Very Short Range Forecasting*, EUMETSAT.

NPD/JMA (1997) *Outline of the Operational Numerical Weather Prediction at Japan Meteorological Agency*, Japan Meteorological Agency.

Tuttle, J. D. & Foote, G. B. (1990) Determination of the boundary layer airflow from a single Doppler radar. *J. Atmos. Ocean. Tech*. **7**: 218–232.

Tuttle, J. D. & Gall, R. (1999) A single-radar technique for estimating the winds in tropical cyclone. *Bull. Am. Meteorol. Soc.* **65**: 653–668.

Wilks, D. S. (1995) *Statistical Methods in the Atmospheric Sciences: An Introduction.* San Diego: Academic Press, 467 pp.

Wilson, J. & Mueller, C. K. (1993) Nowcasts thunderstorm initiation and evolution. *Wea. Forecasting* **8**: 113–131.